Polyphenol–Reduced Graphene Oxide: Mechanism and Derivatization

ARTICLE *in* THE JOURNAL OF PHYSICAL CHEMISTRY C · OCTOBER 2011

Impact Factor: 4.77 · DOI: 10.1021/jp2068683

4 AUTHORS:

Ruijuan Liao
Beijing Institute Of Graphic Communication
8 PUBLICATIONS **165** CITATIONS
SEE PROFILE

Zhenghai Tang
South China University of Technology
32 PUBLICATIONS **445** CITATIONS
SEE PROFILE

Yanda Lei
Howard University
44 PUBLICATIONS **717** CITATIONS
SEE PROFILE

Baochun Guo
South China University of Technology
96 PUBLICATIONS **2,015** CITATIONS
SEE PROFILE

THE JOURNAL OF PHYSICAL CHEMISTRY C

ARTICLE

pubs.acs.org/JPCC

Polyphenol-Reduced Graphene Oxide: Mechanism and Derivatization

Ruijuan Liao,[†] Zhenghai Tang,[†] Yanda Lei,[†] and Baochun Guo*[,†,‡]

[†]Department of Polymer Materials and Engineering and [‡]State Key Laboratory of Pulp and Paper Engineering, South China University of Technology, Guangzhou 510640, China

Supporting Information

ABSTRACT: In this work, tea polyphenols (TPs) were employed as an environmentally friendly and highly efficient reducer and stabilizer for graphene oxide (GO). The results from XPS, Raman, and conductivity studies of reduced graphene indicated the efficient deoxidization of GO. The adsorption of oxidized TPs onto graphene supplies steric hindrance among graphene sheets to keep them individually dispersed in water and some solvents. To investigate the reduction mechanism, epigallocatechin gallate (EGCG), the primary component of TPs, was used as a model. Characterization by ^{1}H NMR and FTIR spectroscopies indicated that the gallic units in EGCG were converted to galloyl-derived orthoquinone and the flavonoid structure survived during the reduction. To further enhance the organosolubility of the resultant graphene, derivatization of the graphene was conducted by galloyl-derived orthoquinone−thiol chemistry. The successful derivatization was found to greatly improve the organosolubility of graphene in solvents with low boiling points.

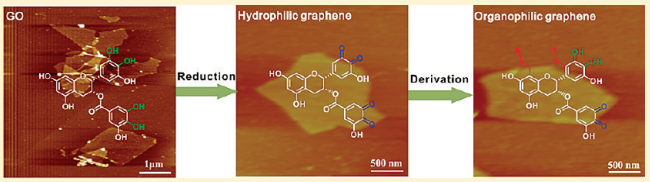

INTRODUCTION

Graphene, a single atomic layer of sp^2-hybridized carbon in a honeycomb crystal lattice, forms one of the strongest in-plane bonds among all materials.[1] Because of its extraordinary properties in electrical, mechanical, and thermal fields, graphene is an ideal material for use in sensors,[2] electrodes,[3,4] and hydrogen storage devices.[5] Also, graphene has been highlighted as a novel component of polymer-based composites. The incorporation of graphene into polymer matrixes has been reported to generate dramatic improvements in properties at very low graphene contents.[6,7]

Graphene can be obtained by many strategies, including chemical vapor deposition (CVD), micromechanical exfoliation of graphite, epitaxial growth on electrically insulating surfaces, and solution-based chemical reduction of graphene oxide (GO).[8−10] However, the first three methods have defects such as difficult preparation, high cost, and low efficiency. Solution-based chemical reduction of GO has been found to be one of the most promising approaches for fabricating graphene on a large scale.[11,12] Because of the analogous structures of chemically reduced GO and pristine graphene, the preparation of graphene by such simple and safe methods is an attractive topic. To date, chemical reducing agents for GO, such as hydrazines,[13,14] alcohols,[15] hydroquinone,[16] vitamin C,[17] sulfur-containing compounds,[18] sodium borohydride,[19] sodium hydroxide,[20] and hydrogen iodide,[21] have been used to remove the hydroxyl and epoxy groups in GO, so that the sp^2 structure and consequent conductive properties can be recovered. The most widely used hydrazines are toxic and corrosive, which poses a persistent obstacle for their applications. The newly emerging reducers such as vitamin C, alcohols, sodium borohydride, sodium hydroxide, and hydrogen iodide are less efficient in deoxidating GO. However, the reduction of GO with these reducers would lead to irreversible aggregation of graphene if no additional stabilizers were used.[15,22−24] Therefore, exploring environmentally friendly reducers that simultaneously act as stabilizers for the reduced GO is highly desired.

Previously, the present authors reported a green reduction process of GO by hydrolyzable tannin (TA).[25] It has been revealed that TA acted as efficient reducing agent and stabilizer simultaneously. Because of the structural similarity, condensed tannins are also believed to be effective to reduce and stabilize GO. Tea polyphenols (TPs), an extract of green tea, comprise a water-soluble mixture of condensed tannins, mainly consisting of four major catechins: (−)-epigallocatechin gallate (EGCG), (−)-epigallocatechin (EGC), (−)-epicatechin gallate (ECG), and (−)-epicatechin (EC). Of these, EGCG accounts for 50−80 wt % of the total catechins in green tea.[26,27] The molecular backbone of TPs is mainly constituted by rigid aromatic rings, which could restrain particle and layer aggregation through their steric hindrance.[28] Actually, Shi et al.[29] recently reported the reduction of GO with a green tea solution. Because of the complex structures of TPs, however, the reduction mechanism of TPs has not been addressed. Herein, we used epigallocatechin gallate (EGCG), the main component of TPs, as a model condensed tannin, to investigate its reduction mechanism toward GO. The resultant TP-decorated graphene (rGO) can be dispersed in various alcohols and some organic solvents with high boiling points such as dimethylformamide (DMF) and *N*-methylpyrrolidone (NMP). However, its organic solubility,

Received: July 18, 2011
Revised: September 9, 2011
Published: September 13, 2011

dx.doi.org/10.1021/jp2068683 | *J. Phys. Chem. C* 2011, 115, 20740–20746

especially in solvents with low boiling points, cannot satisfy processing requirements for the fabrication of graphene-based composites. For a wider spectrum of organic solubility, we functionalized the TP-reduced graphene through nucleophilic addition between galloyl-derived orthoquinones (the oxidized TPs) and thiol.[30,31] The structure and properties of the derivatized rGO (S-rGO) were characterized.

EXPERIMENTAL SECTION

Materials. Natural graphite powder (purity of 99.9%) was produced by Qingdao Xinghua Graphite Co., Ltd., Shandong, China. TPs and EGCG (purity of 98%) were purchased from Xi'an Haoxuan Biotechnology Limited, Xi'an, China. Dodecyl mercaptan (purity of 98%) was purchased from Shanghai Chemical Reagent Company, Shanghai, China. Other chemicals were analytically pure and were used as received.

Preparation of TP-Reduced GO (rGO). GO was prepared by oxidizing natural graphite according to a modified literature method.[32] The rGO colloid was prepared similarly as follows: Typically, GO aqueous solution (1 mg/mL) was prepared by sonication of graphite oxide in water, and then TPs (300 wt % relative to GO) were added. After sonication for 30 min, the mixture was maintained at 80 °C for 8 h. The residual TPs were removed by washing the completed suspension with abundant deionized water and filtering with a nylon membrane (0.22 μm) under a vacuum. This step was performed repeatedly with water in the amount of 15 times the volume of the suspension. During the washing procedure, the color fading of the filtrate indicated the removal of the TPs. After this amount of water, the final filtrate was colorless. rGO sheet was then obtained by vacuum filtration of the above washed suspension through a nylon membrane (0.22 μm). The dried rGO sheet was then peeled off the substrate.

Preparation of Oxidized EGCG (o-EGCG). EGCG was used as the model substance to investigate the reduction mechanism of GO. EGCG (25 wt % relative to GO) was adding to a GO (1 mg/mL) suspension, and the mixture was sonicated for 30 min; then the system was maintained at 80 °C for 8 h. The filtrate, oxidized EGCG (o-EGCG), was collected for further characterization. To exclude thermal effects on the structural changes of EGCG, a similar thermal treatment was applied to EGCG in the absence of GO, and the product (c-EGCG) was subjected to different analyses.

Derivatization of rGO. To obtain a wider spectrum of solubility of rGO in organic solvents, thiol was employed to modify the rGO through nucleophilic addition between galloyl-derived orthoquinone and thiol. Dodecyl mercaptan was selected as the model thiol substance. The thiol-derivatized rGO (S-rGO) was prepared according to the following procedure: Typically, 30 mg of as-prepared rGO was dispersed in 150 mL of ethanol by sonication for 100 min. Then, 30 g of formaldehyde solution (37 wt %), 15 g of dodecyl mercaptan, and 1 g of acetic acid were added to this alcohol suspension. The addition of dodecyl mercaptan to the rGO solution yielded a phase-separated mixture in which rGO remained in the ethanol phase. The mixture was heated at 80 °C for 4 h. After this step, the graphene was extracted into the dodecyl mercaptan phase. One day later, S-rGO remained as a third phase between the ethanol phase and the dodecyl mercaptan phase. The intermediate phase was washed repeatedly with ethanol and dried thoroughly to give the final S-rGO. S-rGO sheet was obtained by filtering the S-rGO solution through a nylon membrane (0.22 μm).

Instruments. X-ray photoelectron spectroscopy (XPS) spectra were obtained on a Kratos Axis Ultra-DLD X-ray photoelectron spectroscope (Manchester, U.K.) with Al Kα radiation of 1486.6 eV. Thermogravimetric analysis (TGA) curves were obtained on a Q5000 apparatus (TA Instruments, New Castle, DE) under a nitrogen atmosphere at a heating rate of 10 °C/min. Raman spectra were measured on a Labram aramis Micro-Raman spectroscope (Jobin Yvon, Villeneuve d'Ascq) using a He laser beam excitation wavelength of 632.8 nm. Electrical conductivity tests were conducted on a Keithley 2635A conductive meter (Solon, OH) using the four-probe method. UV spectra were recorded on a S3150 UV−vis spectrophotometer (Scinco, Seoul, Korea). XRD patterns were recorded on a D8 Advance X-ray diffraction instrument (Bruker, Karlsruhe, Germany). SEM images were acquired on an EVO 18 Special Edition scanning electron microscope (Carl Zeiss, Oberkochen, Germany). FTIR spectra were measured on a Vector 33 FTIR spectrometer (Bruker, Karlsruhe, Germany). ^{1}H NMR spectroscopy were recorded on an MQ20 nuclear magnetic resonance spectrometer (Bruker, Karlsruhe, Germany) with a vibration frequency of 400 MHz. AFM images of GO, rGO, and S-rGO were acquired using a Multimode Nanoscope scanning probe microscope in tapping mode (Veeco, Plainview, NY).

RESULTS AND DISCUSSION

Reduction Mechanism of TPs toward GO. TPs were employed as a kind of highly efficient reducer and stabilizer for GO. The results from XPS, Raman, and conductivity analyses of reduced graphene substantiate the efficient deoxidization of GO by TPs (Table S1 and Figures S1−S4, Supporting Information). The adsorption of oxidized TPs onto graphene supplies steric hindrance among the graphene sheets to keep them stably dispersed in water and some organic solvents.

Because of the complex structure of TPs, the oxidation mechanism of TPs is very complicated and depends on the oxidizer type and oxidization conditions. In the present work, GO acts as a special oxidation agent for TPs. We intend to reveal the structural changes of the basic units of TPs. For clarity, epigallocatechin gallate (EGCG), the main component of TPs, was utilized as a model condensed tannin to reveal the reduction mechanism of TPs toward GO. EGCG was oxidized by excess GO at 80 °C for 8 h, and the oxidized product is denoted o-EGCG. The control sample, c-EGCG, was also prepared as described in the Experimental Section. To reveal the structural changes of o-EGCG and c-EGCG compared with the original EGCG, FTIR and ^{1}H NMR spectroscopic analyses were performed.

The oxidization process of EGCG has been revealed to be very complicated, with the structure of the products depending on different factors including oxidizer nature, pH value, and subsequent coupling reactions.[33,34] However, some common characteristics of oxidized EGCG have been reported in the literature. For example, compared with the ring A, the gallic acid units (including ring B and ring C) in EGCG are much more susceptible toward oxidizers. The oxidation of EGCG generally yields the galloyl-derived orthoquinone. Figure 1 presents the FTIR spectra of EGCG, c-EGCG, and o-EGCG. Based on a comparison with the spectrum of EGCG, the emerging absorptions at 1720 and 2464 cm^{-1} in o-EGCG are assigned to the

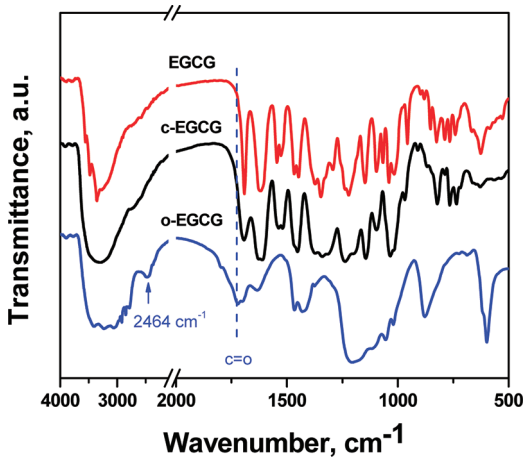

Figure 1. FTIR spectra of EGCG, c-EGCG, and o-EGCG.

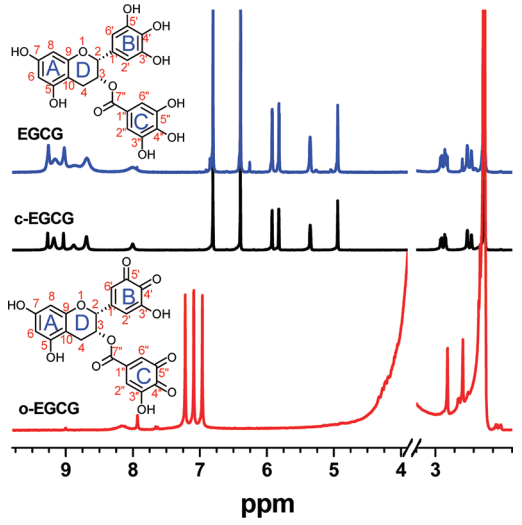

Figure 2. ^{1}H NMR spectra of EGCG, c-EGCG, and o-EGCG.

stretching vibration of C═O and cumulative double bond, clearly indicating the formation of the galloyl-derived orthoquinone structure in o-EGCG. However, there is no substantial difference between the spectra of c-EGCG and EGCG. Thus, it is rational to conclude that the orthoquinone structure in o-EGCG is the product of the oxidation of EGCG by GO, rather than thermal effects.

The formation of EGCG quinone is further substantiated by ^{1}H NMR spectroscopy. Figure 2 depicts the comparison of ^{1}H NMR spectra of EGCG, c-EGCG, and o-EGCG. The assignments of the ^{1}H NMR chemical shifts (δ) of EGCG for ring A (H-6, -8 at δ_H 5.92 and 5.82 s), ring B (H-2′, -6′ at δ_H 6.4 s; OH-3′, -5′ at δ_H 8.69 s; OH-4′ at δ_H 8.00 s), ring C (H-2″, -6″ at δ_H 6.81 s; OH-3″, -5″ at δ_H 9.12 s; OH-4″ at δ_H 8.69 s), and ring D (H-2, -3, -4a, -4e at δ_H 4.94 s, 5.35 s, 2.90 m, and 2.62 d) could be made according to the reported data.[30,35−41] Again, no visible changes can be detected between the spectra of EGCG and c-EGCG, suggesting that the structural characteristics of EGCG survived during the thermal process in the absence of GO. Comparison of the spectra of EGCG and o-EGCG reveals that the most significant characteristic in o-EGCG is the emerging of signals in the range of 6.9−7.3 ppm that can be attributed to the

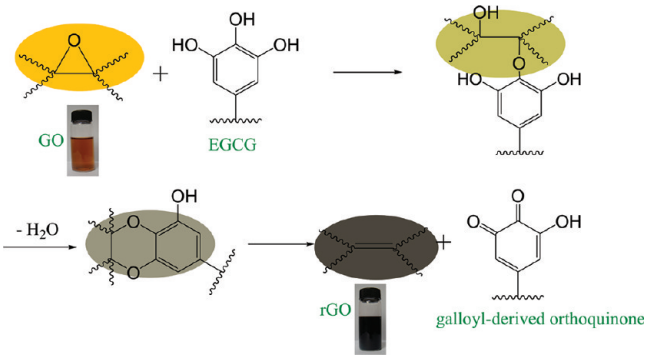

Figure 3. Proposed reduction mechanism of GO by EGCG.

protons in aromatic skeleton at rings A−C. Some of the phenol groups (7.93 ppm) are still observed, which might be due to the presence of phenols in the galloyl-derived orthoquinone and the possible coupling reaction products that can regenerate phenols.[33] In addition, the flavonoid structure (ring D) is not broken, as indicated by the presence of the peaks at 2.71 and 2.87 ppm, although they are slightly shifted compared with those in EGCG.

GO shows a distinct capability to oxidize EGCG so that most of the phenols on the gallic acid units (rings B and C) are converted to galloyl-derived orthoquinone and the flavonoid structure (ring D) survives during the oxidization. The reduction of GO could proceed through the possible mechanism described in Figure 3. First, EGCG is ready to dissociate two protons, functioning as a nucleophile. GO mainly contains different oxygen groups, such as epoxide, hydroxyl, and carboxyl. Most of the epoxide groups, which reside within the plane of GO, are believed to be removed during the oxidation. The opening of the epoxide can be realized by the oxygen anion of EGCG through an S_N2 nucleophilic attack. Then, another backside S_N2 nucleophilic attack leads to the formation of an intermediate, accompanied by the release of H_2O. The subsequent thermal elimination of the intermediate leads to the formation of reduced graphene and galloyl-derived orthoquinone. Zhang et al. suggested a similar S_N2 nucleophilic addition process of epoxide of GO by vitamin C.[22] As shown in Figure 3, the aqueous GO is light brown. After reduction, it becomes black, suggesting the successful reduction of GO.

Derivatization of rGO by Thiol. Although TPs show distinct reducing and stabilizing effects toward GO, the obtained rGO does not show solubility in ketone and ester solvents with low boiling points. For practical applications, such as polymer-based composites, a wider spectrum of solubility is essential. Consequently, the derivatization of rGO was conducted to enhance its soubility. The derivatization chemistry is based on two reactive sites of the galloyl-derived orthoquione. One is the H8 on ring A of the galloyl-derived orthquinone, which undergoes reaction with formaldehyde to form an unstable dimer, followed by decomposition and addition of the thiol to form the sulfide.[31] The other site is H6′ of ring B or H6″ of ring C of the galloyl-derived orthoquinone, which reacts with thiol-based nucleophiles to form another kind of sulfide.[42] The derivatization chemistry is schematically shown in Figure 4a. In the present study, dodecyl mercaptan was used as the model thiol to fulfill the modification of rGO by the described route.

To obtain structural information and confirm the conjugation of TPs with rGO, FTIR and ^{1}H NMR spectroscopies were

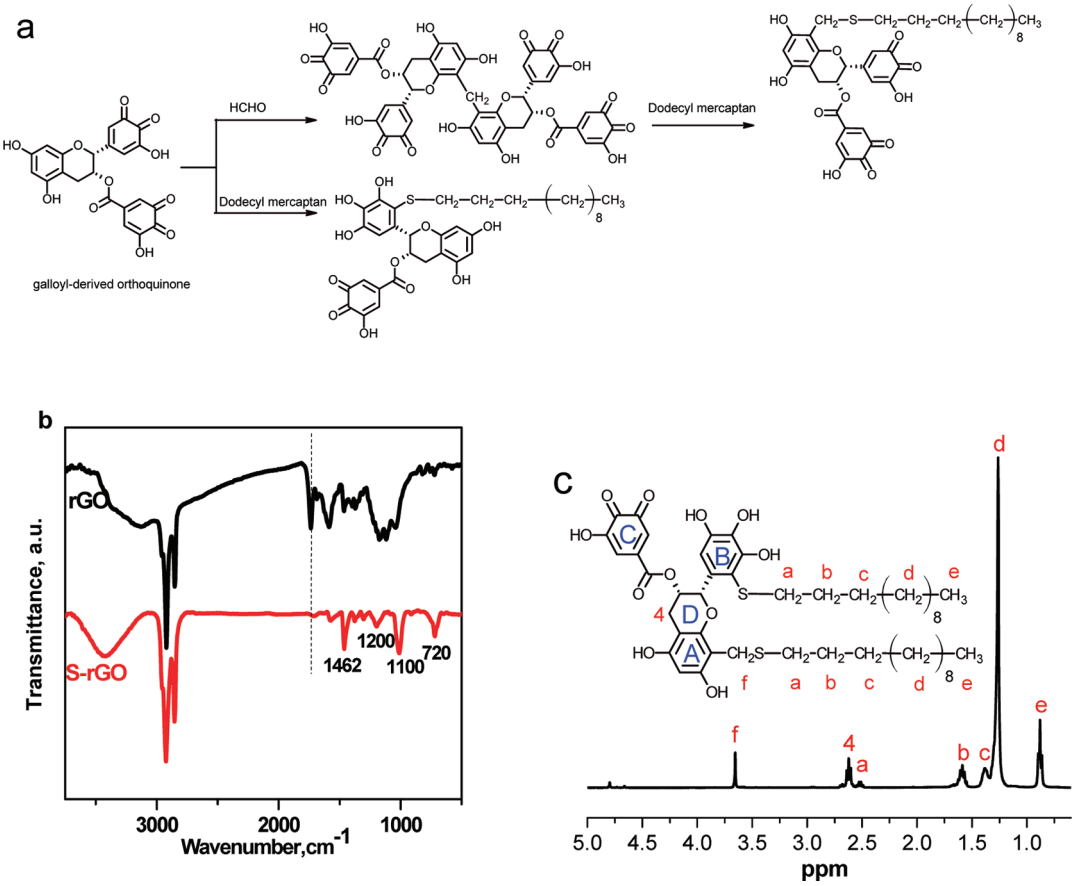

Figure 4. (a) Reaction process of rGO derivatization and (b) FTIR and (c) ^{1}H NMR spectra of S-rGO.

performed on S-rGO. As presented in Figure 4b, the characteristic peak at 1740 cm^{-1} in rGO is attributed to the stretching vibration of C═O of the capped oxidized TPs. However, in the spectrum of S-rGO, it is obvious that this absorption is weakened, suggesting that nucleophilic addition reactions have consumed the C═O groups. The reaction between the galloyl-derived orthoquinone and thiol can regenerate phenols (pyrogallol). Thus, nucleophilic addition reactions have consumed the C═O groups in the quinone, and the C═O is converted into Ar−OH (pyrogallol sulfide). The absorption peak at 720 cm^{-1} originates from the rocking vibration of CH_2 adjacent to the sulfur atom in the sulfides.[43] The absorption peaks 1462 and 1200 cm^{-1} can be assigned to CH_2−S−C deformation and CH_2−S wagging, respectively. These observations suggest the formation of an Ar−CH_2−S− sulfide structure. In addition, a peak is observed around 1100 cm^{-1}, indicating the presence of an Ar−S− sulfide structure. All of these observations support the notion that the addition reaction between dodecyl mercaptan and rGO has taken place, yielding sulfides of the Ar−CH_2−S− and Ar−S− structures.[44] Tentative assignments of ^{1}H NMR spectra of S-rGO (H-a, -b, -c, -d, -e, -f, -4, and -6 at δ_H 2.52 m, 1.59 m, 1.38 s, 1.26 s, 0.88 m, 3.66 s, 2.62 m, and 4.80 s, respectively) were made by comparison with EGCG and literature data.[30,41,45] Particularly, δ_H at 3.66 represents the H on the carbon atom between dodecyl mercaptan and o-EGCG. Clearly, the thiol−TPs linkage through methylene is confirmed. Before such derivatization, rGO is soluble in only ethanol and insoluble in dodecyl mercaptan. After the derivatization, S-rGO is extracted from alcohol into the dodecyl mercaptan phase. One day later, S-rGO remains a third phase between the ethanol and dodecyl mercaptan phases (Figure S5, Supporting Information).

Figure 5 shows a comparison of the solubilities of rGO and S-rGO in various organic solvents. The fully dried rGO can stably be dissolved in NMP, DMF, and most of the alcohols (except for isopropyl alcohol). However, rGO cannot be dissolved in the esters, toluene, and haloalkanes. Also, it cannot be stably dissolved in the ketones, dimethyl sulfoxide (DMSO), tetrahydrofuran (THF), and isopropyl alcohol, although it can be suspended in the ketones and isopropyl alcohol for several hours. It is clear that the derivatization of rGO can improve the solubility significantly in organic solvents, including DMF, NMP, dichloromethane, all of the esters, most of the alcohols (except for the glycols), and all of the ketones, even after standing for 1 month. It was tested that S-rGO can be dissolved in monohydric alcohols such as methanol, ethanol, and isopropanol. Although S-rGO can be dissolved in glycols such as ethylene glycol and propanediol, the S-rGO suspensions in glycols are stable for only several days. We suppose that this difference is caused by the larger molecular size of the glycols. After the derivatization, some of the hydroxyls of the original rGO are covered by lipophilic alkyls. Therefore, the glycols with larger molecular size cannot wedge into the decorated graphene sheet as effectively as the smaller alcohols do. Consequently, S-rGO cannot be stably dispersed in the glycols. Still, S-rGO cannot be dissolved in toluene, DMSO, and THF. Interestingly, it can be

dx.doi.org/10.1021/jp2068683 |J. Phys. Chem. C 2011, 115, 20740–20746

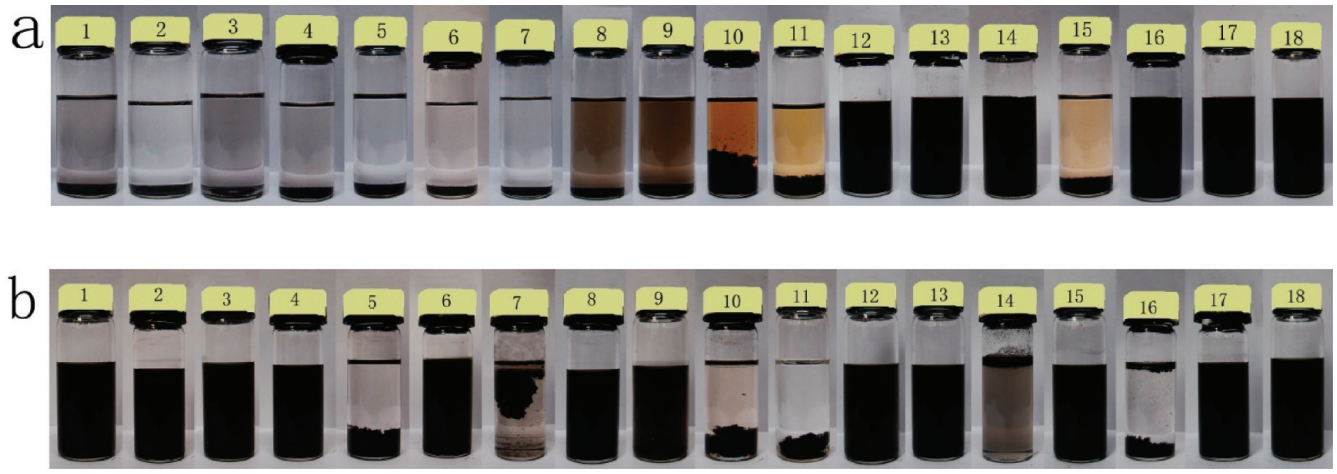

Figure 5. Photographs of (a) rGO and (b) S-rGO dispersions in different solvents (0.5 mg/mL) after 1 month of standing: (1) butyl methacrylate, (2) methyl acrylate, (3) butyl acrylate, (4) ethyl acetate, (5) toluene, (6) dichloromethane, (7) chloroform, (8) acetone, (9) butanone, (10) DMSO, (11) THF, (12) methanol, (13) ethanol, (14) ethylene glycol, (15) isopropanol, (16) propanediol, (17) DMF, and (18) NMP.

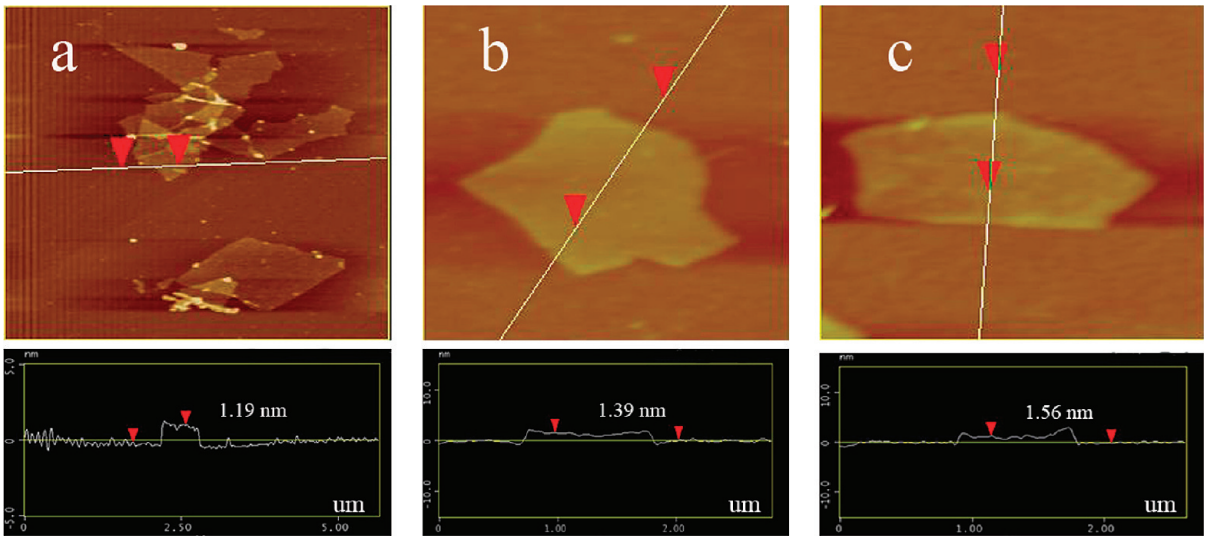

Figure 6. AFM images of (a) GO in water, (b) rGO in water, and (c) S-rGO in dichloromethane.

seen by polarized optical microscopy (POM) that solution aggregates of S-rGO in chloroform (Figure S6, Supporting Information) exhibit crystal-like structures. This is different from rGO, which is completely insoluble in chloroform and ester solvents. We suggest that an ordered crystallized structure of S-rGO might form in chloroform, although further investigation is needed to understand the intrinsic mechanism.

To identify whether the rGO and S-rGO sheets remain isolated or become aggregated, AFM was performed on GO, rGO, and S-rGO. For AFM measurements, a droplet of each of the corresponding colloids (GO and rGO in water and S-rGO in dichloromethane) was deposited on mica and evaporated at room temperature. Figure 6 shows typical AFM images of GO, rGO, and S-rGO sheets and the corresponding height profiles. The thickness of the GO sheets is about 1.19 nm, with lateral sizes of submicrometers to micrometers, indicating the existence of a single-layer GO sheet. For rGO and S-rGO, the thicknesses are 1.39 and 1.56 nm, respectively, which are larger than that of GO. Considering the adsorption of oxidized TPs and derivatized TPs onto graphene platelet, one might expect the rGO and S-rGO sheets to all be individually dispersed in their colloids. It should be emphasized that, in the suspended rGO and S-rGO colloids, no further stabilizers were used. That is, TPs are capable of both reducing GO and stabilizing graphene. After the facile derivatization process, a wider spectrum of solubility of graphene was achieved. The stabilization mechanisms are proposed to be $\pi-\pi$ interactions and hydrogen bonding between the reducer and the graphene layer.[25,29] Further, the capped TPs or their derivatives supply steric hindrance to stabilize the graphene sheets.

The S-rGO sheet maintained a layered structure and was even more flexible than the rGO sheet (Figure S7, Supporting Information). Because of the derivatization, S-rGO was covered with moieties of dodecyl mercaptane, leading to an increase in the *d* spacing between adjacent graphene layers (from 0.34 to 0.43 nm) and a decrease in the sp^2 C═C fraction (from 0.67 to 0.46), which can be calculated from the XRD and XPS spectra, respectively (Figures S8 and S9, Supporting Information).

dx.doi.org/10.1021/jp2068683 |*J. Phys. Chem. C* 2011, 115, 20740–20746

However, this does not have a significant effect on the electrical conductivity of the graphene sheet. The electrical conductivity of S-rGO (1380 S/m) is on the same order of magnitude as that of rGO (2385 S/m). According to the TGA curves of rGO and S-rGO (Figure S10, Supporting Information), the amount of grafted dodecyl mercaptan on S-rGO was calculated to be 31.7%. Such a high grafting yield leads to the significantly changed organosolubility of rGO, which is the main reason for enhanced solubility in various polar solvents.

CONCLUSIONS

As a type of environmentally friendly, low-cost, plant-derived substance, TPs have been demonstrated to be an effective reducer for GO. The TP-reduced graphene can be well-dispersed in water, alcohols, and some polar solvents. The reduction mechanism was revealed by using EGCG as a model reducer. The gallic units (rings B and C) in EGCG were converted to galloyl-derived orthoquinone through nucleophilic addition of epoxide on GO. The flavonoid structure (ring D) survived during the oxidization by GO. The derivatization of rGO aimed at improved solubility was conducted successfully based on galloyl-derived orthoquinone−thiol chemistry. The derivatization of rGO essentially did not sacrifice the electrical conductivity. S-rGO exhibited excellent organosolubility, which broadens the available techniques for fabricating graphene-based materials.

ASSOCIATED CONTENT

Supporting Information. Discussion of the reduction regularity of TP-reduced rGO; photographs of S-rGO before and after the thiol−phenol reaction; SEM images and photographs of rGO and S-rGO; POM image of aggregated S-rGO in chloroform; and XRD patterns, XPS spectra, and TGA curves of S-rGO. This material is available free of charge via the Internet at http://pubs.acs.org.

AUTHOR INFORMATION

Corresponding Author
*E-mail: psbcguo@scut.edu.cn.

ACKNOWLEDGMENT

This work was supported by the National Natural Science Foundation of China (50873035 and 50933001), Fundamental Research for the Central Universities (2009ZZ0007), and Program for New Century Excellent Talents in University (NCET-10-0393).

REFERENCES

(1) Bao, Q. L.; Zhang, H.; Wang, Y.; Ni, Z. H.; Yan, Y. L.; Shen, Z. X.; Loh, K. P.; Tang, D. Y. *Adv. Funct. Mater.* **2009**, *19*, 3077–3083.
(2) Kang, X.; Wang, J.; Wu, H.; Aksay, I. A.; Liu, J.; Lin, Y. *Biosens. Bioelectron.* **2009**, *25*, 901–905.
(3) Li, F. H.; Chai, J.; Yang, H. F.; Han, D. X.; Niu, L. *Talanta* **2010**, *81*, 1063–1068.
(4) Su, C. Y.; Xu, Y. P.; Zhang, W. J.; Zhao, J. W.; Tang, X. H.; Tsai, C. H.; Li, L. J. *Chem. Mater.* **2009**, *21*, 5674–5680.
(5) Geim, A. K.; Novoselov, K. S. *Nat. Mater.* **2007**, *6*, 183–191.
(6) Liang, J. J.; Huang, Y.; Zhang, L.; Wang, Y.; Ma, Y. F.; Guo, T. Y.; Chen, Y. S. *Adv. Funct. Mater.* **2009**, *19*, 2297–2302.
(7) Kuilla, T.; Bhadra, S.; Yao, D.; Kim, N. H.; Bose, S.; Lee, J. H. *Prog. Polym. Sci.* **2010**, *35*, 1350–1375.
(8) Novoselov, K. S.; Geim, A. K.; Morozov, S. V.; Jiang, D.; Zhang, Y.; Dubonos, S. V.; Grigorieva, I. V.; Firsov, A. A. *Science* **2004**, *306*, 666–669.
(9) Berger, C.; Song, Z. M.; Li, X. B.; Wu, X. S.; Brown, N.; Naud, C.; Mayou, D.; Li, T. B.; Hass, J.; Marchenkov, A. N.; Conrad, E. H.; First, P. N.; de Heer, W. A. *Science* **2006**, *312*, 1191–1196.
(10) Dreyer, D. R.; Park, S.; Bielawski, C. W.; Ruoff, R. S. *Chem. Soc. Rev.* **2010**, *39*, 228–240.
(11) Zhang, J. L.; Yang, H. J.; Shen, G. X.; Cheng, P.; Zhang, J. Y.; Guo, S. W. *Chem. Commun.* **2010**, *46*, 1112–1114.
(12) Park, S.; Ruoff, R. S. *Nat. Nanotechnol.* **2009**, *4*, 217–224.
(13) Gao, X. F.; Jang, J.; Nagase, S. *J. Phys. Chem. C* **2010**, *114*, 832–842.
(14) Li, D.; Muller, M. B.; Gilje, S.; Kaner, R. B.; Wallace, G. G. *Nat. Nanotechnol.* **2008**, *3*, 101–105.
(15) Dreyer, D. R.; Murali, S.; Zhu, Y. W.; Ruoff, R. S.; Bielawski, C. W. *J. Mater. Chem.* **2011**, *21*, 3443–3447.
(16) Wang, G. X.; Yang, J.; Park, J.; Gou, X. L.; Wang, B.; Liu, H.; Yao, J. *J. Phys. Chem. C* **2008**, *112*, 8192–8195.
(17) Fernandez-Merino, M. J.; Guardia, L.; Paredes, J. I.; Villar-Rodil, S.; Solis-Fernandez, P.; Martinez-Alonso, A.; Tascon, J. M. D. *J. Phys. Chem. C* **2010**, *114*, 6426–6432.
(18) Chen, W. F.; Yan, L. F.; Bangal, P. R. *J. Phys. Chem. C* **2010**, *114*, 19885–19890.
(19) Shin, H. J.; Kim, K. K.; Benayad, A.; Yoon, S. M.; Park, H. K.; Jung, I. S.; Jin, M. H.; Jeong, H. K.; Kim, J. M.; Choi, J. Y.; Lee, Y. H. *Adv. Funct. Mater.* **2009**, *19*, 1987–1992.
(20) Fan, X. B.; Peng, W. C.; Li, Y.; Li, X. Y.; Wang, S. L.; Zhang, G. L.; Zhang, F. B. *Adv. Mater.* **2008**, *20*, 4490–4493.
(21) Pei, S.; Zhao, J.; Du, J.; Ren, W.; Cheng, H. *Carbon* **2010**, *48*, 4466–4474.
(22) Gao, J.; Liu, F.; Liu, Y. L.; Ma, N.; Wang, Z. Q.; Zhang, X. *Chem. Mater.* **2010**, *22*, 2213–2218.
(23) Fan, Z. J.; Wang, K.; Wei, T.; Yan, J.; Song, L. P.; Shao, B. *Carbon* **2010**, *48*, 1686–1689.
(24) Lomeda, J. R.; Doyle, C. D.; Kosynkin, D. V.; Hwang, W. F.; Tour, J. M. *J. Am. Chem. Soc.* **2008**, *130*, 16201–16206.
(25) Lei, Y. D.; Tang, Z. H.; Liao, R. J.; Guo, B. C. *Green Chem.* **2011**, *13*, 1655–1658.
(26) Khanbabaee, K.; van Ree, T. *Nat. Prod. Rep.* **2001**, *18*, 641–649.
(27) Pelillo, M.; Bonoli, M.; Biguzzi, B.; Bendini, A.; Toschi, T. G.; Lercker, G. *Food Chem.* **2004**, *87*, 465–470.
(28) Huang, X.; Wu, H.; Liao, X. P.; Shi, B. *Green Chem.* **2010**, *12*, 395–399.
(29) Wang, Y.; Shi, Z. X.; Yin, J. *ACS Appl. Mater. Interfaces* **2011**, *3*, 1127–1133.
(30) Sang, S. M.; Lambert, J. D.; Hong, J.; Tian, S. Y.; Lee, M. J.; Stark, R. E.; Ho, C. T.; Yang, C. S. *Chem. Res. Toxicol.* **2005**, *18*, 1762–1769.
(31) Tanaka, T.; Kusano, R.; Kouno, I. *Bioorg. Med. Chem. Lett.* **1998**, *8*, 1801–1806.
(32) Hummers, W., Jr.; Offeman, R. *J. Am. Chem. Soc.* **1958**, *80*, 1339–1339.
(33) Bors, W.; Michel, C.; Stettmaier, K. *Arch. Biochem. Biophys.* **2000**, *374*, 347–355.
(34) Valcic, S.; Burr, J. A.; Timmermann, B. N.; Liebler, D. C. *Chem. Res. Toxicol.* **2000**, *13*, 801–810.
(35) Charlton, A. J.; Haslam, E.; Williamson, M. P. *J. Am. Chem. Soc.* **2002**, *124*, 9899–9905.
(36) Chen, P.; Tan, Y.; Sun, D.; Zheng, X.-M. *J. Zhejiang Univ. Sci.* **2003**, *4*, 714–718.
(37) Palermo, C. M.; Hernando, J. I. M.; Dertinger, S. D.; Kende, A. S.; Gasiewicz, T. A. *Chem. Res. Toxicol.* **2003**, *16*, 865–872.
(38) Lo, C. Y.; Li, S. M.; Tan, D.; Pan, M. H.; Sang, S. M.; Ho, C. T. *Mol. Nutr. Food Res.* **2006**, *50*, 1118–1128.
(39) Xu, J.; Sandstrom, C.; Janson, J. C.; Tan, T. *Chromatographia* **2006**, *64*, 7–11.

(40) Gradisar, H.; Pristovsek, P.; Plaper, A.; Jerala, R. *J. Med. Chem.* **2007**, *50*, 264–271.
(41) Han, D. W.; Matsumura, K.; Kim, B.; Hyon, S. H. *Bioorg. Med. Chem.* **2008**, *16*, 9652–9659.
(42) Quideau, S.; Feldman, K. S.; Appel, H. M. *J. Org. Chem.* **1995**, *60*, 4982–4983.
(43) Sakakibara, M.; Harada, I.; Matsuura, H.; Shimanouchi, T. *J. Mol. Struct.* **1978**, *49*, 29–42.
(44) *AIST RIO-DB Spectral Database for Organic Compounds (SDBS)*, http://riodb01.ibase.aist.go.jp/sdbs/cgi-bin/direct_frame_top.cgi, National Institute of Advanced Industrial Science and Technology (AIST): Tokyo, Japan, 2004.
(45) Hu, Y. H.; Chen, C. Y.; Wang, C. C.; Huang, Y. H.; Wang, S. P. *J. Polym. Sci. A: Polym. Chem.* **2004**, *42*, 4976–4993.